Thermal and Photochemical Reactions of Methylrhenium Diperoxide: Formation of Methyl Hydroperoxide in Acetonitrile

Wei-Dong Wang and James H. Espenson*

Department of Chemistry, Iowa State University, Ames, Iowa 50011

Received May 30, 1997[⊗]

Compared to the system in aqueous solution, the equilibration reactions in acetonitrile between MTO and the methylrhenium peroxides $CH_3ReO_2(\eta^2\text{-}O_2)$ (**A**) and $CH_3ReO(\eta^2\text{-}O_2)_2(H_2O)$ (**B**) are slower but more favored thermodynamically. In CH_3CN, small concentrations of water facilitate the formation of **A** (especially) and **B**. These species decompose to methyl hydroperoxide and perrhenic acid in CD_3CN, rather than to methanol and perrhenic acid as in aqueous solution. The proposed mechanism involves the intramolecular migration of the methyl group to a peroxo oxygen, followed by hydrolysis, and it is facilitated by photolysis. The potential use of **B** as photocatalyst does not seem promising, however.

Introduction

Transition metal peroxo complexes, particularly those containing d^0 metals such as Ti^{IV}, V^V, Cr^{VI}, Mo^{VI}, and W^{VI}, play an important role in catalytic oxo-transfer reactions.[1,2] Recently, attention has especially been devoted to another d^0 compound, methylrhenium trioxide (CH_3ReO_3, abbreviated as MTO); with H_2O_2 this system exhibits high reactivity and catalytic activity. MTO has been shown to activate H_2O_2 by formation of two peroxo compounds, $CH_3ReO_2(\eta^2\text{-}O_2)$ (**A**) and $CH_3ReO(\eta^2\text{-}O_2)_2(H_2O)$ (**B**), eq 1.[3,4]

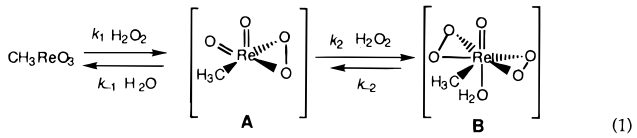

(1)

The coordinated peroxide groups can transfer an oxygen atom to a wide range of substrates, such as alkenes,[5,6] halides,[7,8] organonitrogen species,[9−11] phosphines,[12] and several classes of sulfur-containing compounds.[13−15] Equation 2, using **A** as an example, illustrates the versatility of this catalytic oxo-transfer system. Kinetic studies have revealed a common mechanism for those oxygen atom transfer reactions which involves the nucleophilic attack by a given substrate X on a peroxide oxygen of **A** and **B**.[6,12,14]

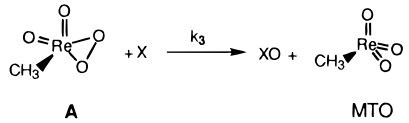

X = alkenes, halides, phosphines, N- and S-containing species (2)

The thermal reactions of transition metal peroxides have been studied extensively with only limited reports of photochemical reactions. The photochemistry of organometallic oxides and peroxides containing d^0 transition metals remains in a formative stage.[16−19] It has been shown that $L_nCo^{III}(\mu\text{-}\eta^1\text{:}\eta^1\text{-}O_2)Co^{III}L_n$ complexes undergo intramolecular ligand (peroxo) to metal charge-transfer reactions upon photolysis, resulting in dissociation and decomposition.[20] Photolysis of complexes of the type $L_nM(\eta^2\text{-}O_2)_{1-2}$ usually generates molecular oxygen, in certain cases in its electronically excited singlet state.[19−24] Although certain photochemical studies of MTO and **B** have appeared,[16,17,19] we have investigated the photochemistry of **B**, which absorbs at 300−450 nm. Studies of the thermal equilibrium and decomposition of the MTO−H_2O_2 system in acetonitrile and of the photochemical reactions of **B** have been carried out to learn the reactions occurring and to define their mechanisms.

[⊗] Abstract published in *Advance ACS Abstracts,* October 1, 1997.

(1) Kitajima, N.; Akita, M.; Moro-oka, Y. Transition metal peroxides and related compounds. In *Organic Peroxides*; John Wiley & Sons: Chichester, 1992; p 535.
(2) Conte, V.; Di Furia, F.; Modena, G. Transition metal catalyzed oxidation. The role of peroxometal complexes. In *Organic Peroxides*; John Wiley & Sons: Chichester, 1992; p 559.
(3) Herrmann, W. A.; Fischer, R. W.; Scherer, W.; Rauch, M. U. *Angew. Chem., Int. Ed. Engl.* **1993**, *32*, 1157.
(4) Yamazaki, S.; Espenson, J. H.; Huston, P. *Inorg. Chem.* **1993**, *32*, 4683.
(5) Herrmann, W. A.; Fischer, R. W.; Marz, D. W. *Angew. Chem., Int. Ed. Engl.* **1991**, *30*, 1638.
(6) Al-Ajlouni, A. M.; Espenson, J. H. *J. Am. Chem. Soc.* **1995**, *117*, 9243.
(7) Espenson, J. H.; Pestovsky, O.; Houston, P.; Staudt, S. *J. Am. Chem. Soc.* **1994**, *116*, 2869.
(8) Hansen, P. J.; Espenson, J. H. *Inorg. Chem.* **1995**, *34*, 5839.
(9) Zhu, Z.; Espenson, J. H. *J. Org. Chem.* **1995**, *60*, 1326.
(10) Murray, R. W.; Iyanar, K.; Chen, J.; Waring, J. T. *Tetrahedron Lett.* **1996**, *37*, 805.
(11) Goti, A.; Nannelli, L. *Tetrahedron Lett.* **1996**, *37*, 6025.
(12) Abu-Omar, M. M.; Espenson, J. H. *J. Am. Chem. Soc.* **1995**, *117*, 272.
(13) Huston, P.; Espenson, J. H.; Bakac, A. *Inorg. Chem.* **1993**, *32*, 4517.
(14) Vassell, K. A.; Espenson, J. H. *Inorg. Chem.* **1994**, *33*, 5491.
(15) Adam, W.; Mitchell, C. M.; Saha-Moller, C. R. *Tetrahedron* **1994**, *50*, 13121.
(16) Kunkely, H.; Turk, T.; Teixeira, C.; Bellefon, C. M.; Herrmann, W. A.; Vogler, A. *Organometallics* **1991**, *10*, 2090.
(17) Herrmann, W. A.; Kühn, F. E.; Fiedler, D. A.; Mattner, M. R.; Geisberger, M. R.; Kunkely, H.; Vogler, A.; Steenken, S. *Organometallics* **1995**, *14*, 5377.
(18) Kunkely, H.; Vogler, A. *J. Photochem. Photobiol. A: Chem.* **1996**, *94*, 135.
(19) Hatzopoulos, I.; Brauer, H.-D.; Geisberger, M.; Herrmann, W. A. *J. Organomet. Chem.* **1996**, *520*, 201.
(20) Ledon, H.; Bonnet, M. *J. Chem. Soc., Chem. Commun.* **1979**, 702.
(21) Vogler, A.; Kunkely, H. *J. Am. Chem. Soc.* **1981**, *103*, 6222.
(22) Seip, M.; Brauer, H.-D. *J. Photochem. Photobiol. A: Chem.* **1993**, *76*, 1.
(23) Hoshino, M.; Yamamoto, K.; Lillis, J. P.; Chijimatsu, T.; Uzawa, J. *Inorg. Chem.* **1993**, *32*, 5002.
(24) Kwong, D. W. J.; Chan, O. Y.; Wong, R. N. S.; Musser, S. M.; Vaca, L.; Chan, S. L. *Inorg. Chem.* **1997**, *36*, 1276.

S0020-1669(97)00650-2 CCC: $14.00

Experimental Section

Materials. Methylrhenium trioxide, CH_3ReO_3 (Aldrich), H_2O_2 (30%, Fisher, standardized by iodometric titration), CF_3COOH (Aldrich), $HClO_4$ (Fisher), PPh_3 (Aldrich), $(CH_3O)_2SO_2$ (Kodak), KOH (Fisher), CH_3CN (Fisher), CD_3CN (CIL), and CD_2Cl_2 (CIL) were used as received. The compound CH_3OReO_3 was prepared according to literature procedure.[25] Its ^{1}H-NMR resonance in CD_3CN at room temperature was broad. The identity of CH_3OReO_3 was further assured by converting it to a more thermally stable chelated species by adding $(CH_3)_2NCH_2CH_2N(CH_3)_2$ to CH_3OReO_3 in THF. High-purity H_2O was obtained by passing laboratory distilled water through a Millipore-Q water purification system.

Kinetic Studies. Kinetic data for the formation of **A** and **B** in CH_3CN were collected by following the absorbance changes at 320 or 360 nm, the maxima for **A** ($\epsilon_{320} = 700$ L mol^{-1} cm^{-1}) and **B** ($\epsilon_{360} = 1200$ L mol^{-1} cm^{-1}). Shimadzu UV-2101PC or UV-3101PC spectrophotometers equipped with a thermostated cell holder were used. The temperature was controlled at 25.0 ± 0.2 °C, unless otherwise indicated. The reaction occurs in two well-separated stages ($k_f > k_s$), which allowed us to use a biexponential function, eq 3, to fit the biphasic kinetic traces. In eq 3, k_f and k_s represent the pseudo-first-order rate

$$\mathrm{Abs}_t = \mathrm{Abs}_\infty + \alpha e^{-k_f t} + \beta e^{-k_s t} \quad (3)$$

constants for the two stages. The amplitude constants α and β are given by[26]

$$\alpha = \frac{(\epsilon_{\mathbf{A}} - \epsilon_{\mathrm{MTO}})k_f - (\epsilon_{\mathrm{MTO}} - \epsilon_{\mathbf{B}})k_s}{k_s - k_f}[\mathrm{MTO}]_0$$

$$\beta = \frac{(\epsilon_{\mathbf{B}} - \epsilon_{\mathbf{A}})k_f}{k_s - k_f}[\mathrm{MTO}]_0 \quad (4)$$

In some cases an insufficient number of data points were collected in the first component. For them, k_s was obtained by a first-order fit of the latter portion after removing 10 half-lives of the faster component. Then k_f was obtained by inputting that k_s as a constant into eq 3 for the fit of the early stages of the data.

The linear plots of the pseudo-first-order rate constants k_f or k_s vs $[H_2O_2]$ have no intercept, indicating that contributions of the reverse reactions of eq 1 are small, as a result of the equilibrium positions favoring **A** and then **B** at the concentrations used.

Equilibrium constants were determined by integrating the ^{1}H spectrum before *and during* the decomposition process. The decomposition kinetics of **B** in CD_3CN were obtained with ^{1}H-NMR and UV−vis methods. In the NMR measurements H_2O_2 was in ≥20−fold excess over $[MTO]_0$. The disappearance of **B** was also followed spectrophotometrically with $[MTO]_0 \leq 1$ mM. With both techniques the rate constants are the same at a given concentration of H_2O_2. The activation parameters of the decomposition processes were obtained from kinetic data in CH_3CN between 25.0 and 59.3 °C.

Photolysis. To prevent the direct photolysis of H_2O_2 itself, light ($\lambda > 400$ nm) from a 300 W sunlamp was obtained by using two KV-399 filters (Schott, Germany). The temperature was controlled by the use of a small submersible circulating pump with tap water for room-temperature photolysis and with salt−ice water for low temperature (0 to −5 °C) photolysis. Most of the photochemical experiments were carried out in NMR tubes. To minimize the interference from MTO and especially from **A**, the MTO−H_2O_2−substrate solution was kept in the dark for about 30 min to allow for all of the MTO and **A** to be converted to **B**, as verified from the ^{1}H-NMR spectrum. Then this solution was photolyzed along with the control samples, MTO−substrate and H_2O_2−substrate. Meanwhile, the thermal reaction of MTO−H_2O_2−substrate was carried out in the dark. All of the samples were monitored by the use of ^{1}H-NMR spectroscopy.

To determine that O_2 is generated upon photolysis of **B**, a larger scale (5 mL) reaction was carried out in a sealed Pyrex flask. After the yellow color of **B** had faded, argon was passed through the solution and then into basic pyrogallol.[27] A similar experiment was performed for the MTO−H_2O_2 solution in the dark. A UV−vis spectrophotometer was used to quantify the relative amount of O_2 produced. To verify this method, argon was passed through an air- and an oxygen-saturated CH_3CN solution and then into the pyrogallol. Attempts to quantitatively measure O_2 with an oxygen electrode were not successful owing to the nature of the solvent and the oxidizing strength of MTO−H_2O_2.

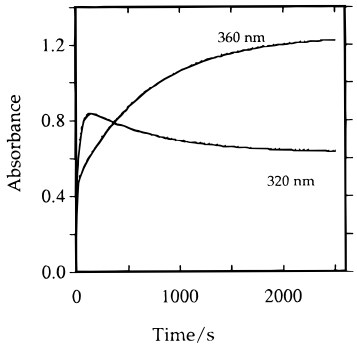

Figure 1. Absorbance−time profiles of the CH_3ReO_3 (1.0 mM)−H_2O_2 system in CH_3CN containing 2.0 M H_2O at 25 °C. Data are shown with 36 mM H_2O_2 at 320 nm, the maximum for **A**, and with 100 mM H_2O_2 at 360 nm, the maximum for **B**.

Product Analysis. The reaction products were characterized by the use of a Bruker DRX-400 spectrometer. ^{1}H and ^{31}P{^{1}H} NMR spectra were recorded at 400.13 and 161.98 MHz, respectively. ^{1}H chemical shifts were measured relative to residual ^{1}H resonance in the deuterated solvents, $CHCl_3$ ($\delta = 7.26$ ppm), $CDHCl_2$ ($\delta = 5.32$ ppm), CD_2HCN ($\delta = 1.94$ ppm). The ^{1}H-NMR spectra of most of the organic products in this study could be compared with the ^{1}H-NMR spectra of authentic samples.

Results

Formation of A and B. As in THF,[3,28] **A** in CH_3CN has a maximum at 320 nm. A kinetics experiment monitored at 320 nm, Figure 1, shows two well-separated stages. The first part with increasing absorbance corresponds to the buildup of **A** whereas the decreasing component results from the transformation of **A** to **B**.[29] Data at 360 nm, which represents the buildup of **B**, is also shown in Figure 1. The biphasic kinetics were analyzed according to eq 3.

For the fast stage, with $[MTO]_0 = 1.0$ mM and the water concentration kept constant at 2.0 M, the plots of k_f and k_s vs $[H_2O_2]$ define lines that pass through the origin; the slopes are $k_1 = 0.81 \pm 0.04$ L mol^{-1} s^{-1} and $k_2 = 0.045 \pm 0.002$ L mol^{-1} s^{-1}. Then, the water content was varied to 2.0 M, with $[MTO]_0 = 1.0$ mM and $[H_2O_2] = 31$ mM; k_f (especially) and k_s rise steeply with $[H_2O]$, Figure 2. Certain experiments were designed to evaluate the rate constant of the slow stage by focusing on data collection at longer times. Such data were therefore less well suited to evaluate the rate constant of the fast stage, as insufficient data were obtained; thus scattered values were obtained. The scatter was particularly pronounced when the concentration of H_2O is high, such that there were not enough data points for the fast stage.

At fixed concentrations of hydrogen peroxide and MTO, 88 and 1.0 mM, the values of k_1 and k_2 were determined over the temperature range 25−59.6 °C. The activation parameters are as follows:

(25) Edeards, P.; Wilkinson, G. *J. Chem. Soc., Dalton Trans.* **1984**, 2695.
(26) Espenson, J. H. *Chemical Kinetics and Reaction Mechanisms*; 2nd ed.; McGraw-Hill: New York, 1995.
(27) Gordon, A. J.; Ford, R. A. *The Chemist's Companion—A Handbook of Practical Data, Techniques, and References*; John Wiley & Sons: New York, 1972.
(28) Abu-Omar, M. M.; Hansen, P. J.; Espenson, J. H. *J. Am. Chem. Soc.* **1996**, *118*, 4966.
(29) We recognize that a rising and falling absorbance will be observed irrespective of which rate constant is the larger; the assignment indicated here is based on additional evidence.

Table 1. Summary of the Rate and Equilibrium Constants for Reaction 1 between CH_3ReO_3 and H_2O_2 in Different Solvents at 25 °C

	in H_2O[a]	CH_3CN:H_2O[c] (1:1)	in CH_3OH[d]	in CH_3CN[e] + 2.6 M H_2O
k_1/L mol^{-1} s^{-1}	80	32.5		0.81 ± 0.04
k_{-1}/s^{-1}	10	3.0		$(3.9 \pm 0.22) \times 10^{-3}$
K_1/L mol^{-1}	7.7 ($\mu = 0.10$) 16.1 ($\mu = 2.0$)[b]	13	261	209 ± 6
k_2/L mol^{-1} s^{-1}	5.2	1.05		0.045 ± 0.002
k_{-2}/s^{-1}	0.04	0.008		$(6.8 \pm 0.72) \times 10^{-5}$
K_2/L mol^{-1}	145 ($\mu = 0.10$)[a] 132 ($\mu = 2.0$)[b]	136	814	660 ± 64

[a] pH = 1.0, ref 4. [b] pH 0, $\mu = 2.0$ M, ref 28. [c] pH = 1.0, ref 12. [d] Reference 9. [e] This work; k_{-1} and k_{-2} were calculated from $K_1 = k_1/k_{-1}$ and $K_2 = k_2/k_{-2}$.

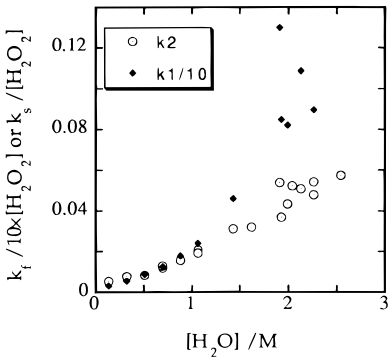

Figure 2. The effect of H_2O on the rate constants k_f and k_s from the biexponential fits to the absorbance−time data. To include data at varying peroxide concentrations, the rate constants were divided by [H_2O_2].

	$\Delta S^{\ddagger}$/J mol^{-1} K^{-1}	$\Delta H^{\ddagger}$/kJ mol^{-1}	k_{298}/L mol^{-1} s^{-1}
k_1	-212 ± 6	24.5 ± 1.9	0.81 ± 0.04
k_2	-214 ± 2	29.0 ± 0.7	0.045 ± 0.002

Equilibrium Constants. In MTO−H_2O_2 solutions in acetonitrile-d_3, the individual methylrhenium species (MTO, **A**, and **B**) could be detected and measured with ^{1}H-NMR. The methyl resonance of **A** is shifted upfield of MTO in CD_3CN, the reverse of their positions in THF-d_8 or CD_3OD. In accord with eq 1, the concentration−time values for **A** and **B** were fitted to biexponential kinetics and [MTO] to first-order kinetics.

During the first 35 min of a reaction with $[H_2O_2]_0 = 140$ mM, $[MTO]_0 = 13$ mM, and $[H_2O] = 2.6$ M (2.1 M added and 0.5 M from hydrogen peroxide), [**A**], after a quite rapid increase, then declined from 8.9 to 0.30 mM and [MTO] from 0.40 to 0.012 mM. K_1 was evaluated at each point, the average being $K_1 = 209 \pm 6$ L mol^{-1}. This constancy confirms that reaction 1 had attained equilibrium before the first reading; as **B** decomposed, the equilibrium was maintained. At $[H_2O_2]_0 = 73$ mM, $K_1 = 249 \pm 16$ L mol^{-1}, the same within the error. A similar procedure was applied to [**A**] and [**B**] values at longer times, 50−5660 min, to calculate $K_2 = 660 \pm 64$ L mol^{-1}. At other peroxide concentrations the K_2 values are 690 (290 mM H_2O_2) and 730 L mol^{-1} (420 mM), seemingly the same within the error. The equilibrium concentration of peroxide was calculated from the mass balance relation in eq 5 that explicitly recognizes its diminution from the formation of methyl hydroperoxide.

$$[H_2O_2]_{eq} = [H_2O_2]_0 - [\mathbf{A}] - 2[\mathbf{B}] - 2[CH_3OOH] \quad (5)$$

The expressions in eq 6 used to calculate the K values do not introduce explicitly the concentration of H_2O, constant at 2.6 M. Table 1 summarizes the equilibrium and rate constants obtained in different solvents. The rate constants of the reverse reactions in eq 1 in CH_3CN were calculated from the equations $k_{-1} = k_1/K_1$ and $k_{-2} = k_2/K_2$.

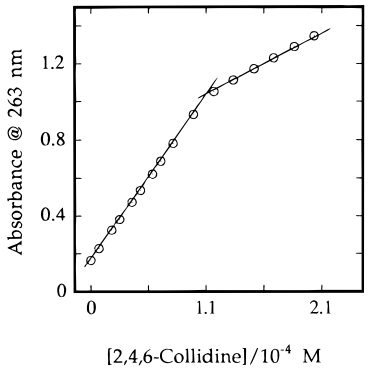

Figure 3. A spectrophotometric titration with 0.012 M 2,4,6-collidine solution in CH_3CN. The perrhenic acid was titrated in a spent solution that initially contained 1.0 mM CH_3OReO_3 and 0.088 M H_2O_2, and which was diluted 8-fold before the titration.

$$K_1 = \frac{[\mathbf{A}]}{[CH_3ReO_3][H_2O_2]} \qquad K_2 = \frac{[\mathbf{B}]}{[\mathbf{A}][H_2O_2]} \quad (6)$$

Formation of $HOReO_3$. The photochemical and thermal decomposition of **B** forms perrhenic acid, easily recognized in the UV spectrum from the unique fine structure of ReO_4^-. It was particularly evident after the excess peroxide had been decomposed with a small amount of MnO_2. The amount of $HOReO_3$ was determined by spectrophotometric titration with 2,4,6-collidine. Aliquots of samples first used for UV−vis and NMR kinetics were diluted and then titrated with a collidine solution in CH_3CN. The amount of acid from the titration corresponds to the initial MTO concentration, allowing us to conclude that perrhenic acid is the only rhenium product. A typical titration graph is given in Figure 3. The method was verified with an authentic $HOReO_3$ sample.

Formation of CH_3OOH and Other Organic Products. In addition to **B** and the signal at δ 3.26 ppm (CH_3OH), a singlet appeared at δ 3.75 ppm in the ^{1}H-NMR upon photolyzing **B** in CD_3CN for 2 h. Unlike the photolysis reaction, the thermal decomposition of **B** in CD_3CN at room temperature was very slow and the predominant product appeared at δ 3.75 ppm, which does not correspond to CH_3OH. This new species has a ^{13}C signal at δ 64.7 ppm, compared with the CH_3OH, δ 49.5 ppm. These two compounds account for >99% of the decomposition products in that the sum of their integrals nearly equals that of the initial CH_3ReO_3. Figure 4 displays these results. Acidifying the spent solution of **B** with $DClO_4$ or CF_3CO_2H did not affect the ratio of these two compounds in weeks. The δ 3.75 ppm species remained unchanged for hours after addition of a ca. 20-fold excess of 2,4,6-collidine, showing that the $HOReO_3$ measured by titration does not arise from the hydrolysis of other rhenium products. Introducing CH_3OCH_3 gave rise to a new singlet at δ 3.24 ppm. The unidentified product is clearly not CH_3OCH_3. The spectroscopic data are, however, in agreement with methyl perrhenate, CH_3OReO_3, or a deriva-

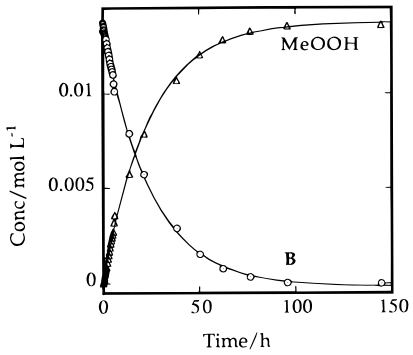

Figure 4. ^{1}H-NMR data for the conversion of CH_3OOH from **B** in CD_3CN. Conditions: $[MTO]_0 = 14$ mM, $[H_2O_2]_0 = 0.75$ M, $[H_2O]_0 = 2.6$ M; 25 °C.

tive; it is ruled out, however, by its chemical properties and by the fact that all of the rhenium was accounted for as perrhenic acid.

Addition of excess PPh_3 converted all of the δ 3.75 ppm species into CH_3OH, perhaps implicating an organic peroxide. Though the NMR data for CH_3OOCH_3 and CH_3OOH are not available in the literature, their likely ^{1}H NMR chemical shifts appear compatible on the basis of Swern's work on other organic peroxides.[30] A convenient published procedure was used to prepare in solution CH_3OOCH_3 and CH_3OOH from dimethyl sulfate and hydrogen peroxide in the presence of potassium hydroxide.[31] The major gas phase product was CH_3OOCH_3, though a small amount of CH_3OCH_3 was also observed. The CD_3CN solution of dimethyl peroxide showed a resonance at δ 3.76 ppm; however, a new signal at δ 3.75 ppm grew in as CH_3ReO_3 and H_2O_2 were added. Again, the δ 3.75 ppm peak transformed to CH_3OH and the CH_3OOCH_3 resonance remained the same upon adding excess PPh_3. The major products of the $(CH_3)_2SO_4-H_2O_2-KOH$ solution upon acidifying with $HClO_4$ were CH_3OOH and $CH_3OSO_3^-$, with NMR signals at δ 3.75 and δ 3.60 ppm, respectively. The CH_3OOH thus prepared reacts with PPh_3 to yield CH_3OH and $Ph_3P{=}O$ on the basis of ^{1}H and $^{31}P\{^1H\}$ NMR spectra. When MTO and H_2O_2 were added to the CH_3OOH solution, the resonance at δ 3.75 increased. Thus all of the evidence indicates that the decomposition product of **B** seen at δ 3.75 ppm is CH_3OOH.

The methyl hydroperoxide formed from **B** is stable at 40 °C for at least 24 h. It slowly decomposes to HCO_2H, $CH_2(OH)_2$, and CH_3OH at elevated temperature. At 60 °C, 36% of CH_3OOH decomposed in 24 h to HCO_2H (20%), $CH_2(OH)_2$ (32%), and CH_3OH (47%). The product distribution was calculated on the basis of integrations of the ^{1}H signals.

As mentioned above, a small amount of CH_3OH was also detected, in an amount that varied with the initial concentration of H_2O_2. The higher the $[H_2O_2]_0$, the less the CH_3OH produced. For example, with $[MTO]_0 = 14$ mM and >20-fold excess of H_2O_2, <6% CH_3OH was formed. However, 20% CH_3OH was found when $[MTO]_0 = 14$ mM and $[H_2O_2]_0 < 0.14$ M. A trace amount of hydrated formaldehyde was also observed, particularly when the $[H_2O_2]_0/[MTO]_0$ was <10.

Kinetics of the Thermal Decomposition of B. The first-order rate constant was determined from spectrophotometric measurements in acetonitrile. At a given [MTO], the rate constant was independent of the initial concentration of hydrogen peroxide. The rate constant was evaluated in experiments in the range 25.0−59.3 °C. The activation parameters are $\Delta H^{\ddagger} = 50$ kJ mol^{-1}, $\Delta S^{\ddagger} = -190$ J mol^{-1} K^{-1}; $k_{298} = 2.1 \times 10^{-6}$ s^{-1}.

Photoinduced Methyl Migration. Irradiation (>400 nm for 5 h) of a sample initially containing 12 mM **B** and 0.65 M H_2O_2 forms 6.8 mM CH_3OH (57%) and 5.2 mM CH_3OOH (43%). Further photolysis for several hours did not change the CH_3OH/CH_3OOH ratio. Under similar conditions in the dark, only 22% of **B** had reacted in 8 h, giving 18% CH_3OOH and 4% CH_3OH. After **B** had completely disappeared in 8 days, nearly 96% of the organic products was CH_3OOH. The methyl hydroperoxide thus formed did not convert to CH_3OH in a week at 25 °C.

The photodecomposition of **B** under oxygen and argon is the same. Adding 0.2 M CH_3OH before photolysis did not affect the rates and product distribution. Similar outcomes have been observed for the thermal decomposition of **B**.

The photolysis of **B** in the absence of excess of H_2O_2 in CH_2Cl_2 at 248−365 nm was reported to give chloromethane, ReO_3, and O_2 under these conditions.[19] We photolyzed **B** (prepared from and in equilibrium with MTO and H_2O_2) in CD_2Cl_2 and detected CH_3OH (δ 3.42 ppm) and CH_3OOH (δ 3.86 ppm) by ^{1}H-NMR.

Photolysis of B in the Presence of Substrates. The photodecomposition of **B** in the presence of benzhydrol derivatives was studied, but it yielded little in the way of new reactions. Most proceeded as before, but a few new organic products were found, especially in an oxygen atmosphere as compared to argon. With 4-methylbenzhydrol,^{1}H-NMR and GC−MS showed benzaldehyde (but only a trace of 4-methylbenzaldehyde) and 3-methylphenol, which were comparable in amount to a ring-oxidized product.

To test for a phenoxyl radical, 2,4,6-triphenylphenol trapping was attempted. No identifiable products resulted. The thermal and photochemical reactions with 1,4-dihydronaphthalene were carried out below 0 °C so that the thermal epoxidation would not interfere. The major photoproduct was naphthalene, but the control (photolysis of hydrogen peroxide with 1,4-dihydronaphthalene) also gave naphthalene.

Photoassisted Formation of O_2. Molecular oxygen was produced in the photolysis of **B** in acetonitrile at λ >400 nm, just as it was in CH_2Cl_2 at 248−365 nm.[19]

Discussion

Equilibrium Constants. Consistent values of the equilibrium constants K_1 and K_2 were obtained at different peroxide concentrations throughout the course of the decomposition process, which is much slower than the equilibration reactions between MTO, **A**, and **B.** The kinetic studies confirmed that also in this medium, as in others, **A** forms faster than **B**. The decomposition of **B** is much slower than the formation of **A** and **B**, allowing the decomposition system to be treated as two fast equilibria and a rate-controlling step.

The values of K_1 and K_2 in CH_3CN are similar to those obtained in CH_3OH. These values are considerably larger than those in water, and the cooperativity effects ($K_2 > K_1$) in CH_3CN and CH_3OH are less pronounced than that in H_2O. The significant difference of equilibrium constants between organic solvents and water may (partially) result from the omission of the activity of water in the equilibrium constant calculation. Nonetheless we would emphasize that such a representation of the thermodynamics is the only reasonable course, given the uncertainty as to whether **A** is the pictured "anhydride" structure or whether it incorporates highly labile water molecule(s), not detected by NMR.[28] These options lead to an unspecified

(30) Swern, D.; Clements, A. H.; Loung, T. M. *Anal. Chem.* **1969**, *41*, 412.
(31) Davies, D. M.; Deary, M. E. *J. Chem. Soc., Perkin Trans. 2* **1992**, 559.

Table 2. Product Distributions from $CH_3ReO_3-H_2O_2$ in Aqueous and Acetonitrile Solutions at 25 °C

	amount of product (%)		
	in H_2O[a]	in CH_3CN	
product	thermal	thermal	photochemical
CH_3OH	100	4	57
CH_3OOH	0	96	43
$HOReO_3$	100	100	100

[a] Reference 28.

number of water molecules on one side or the other of steps 1 *and* 2 in eq 1.

Solvent Effects on Kinetics. Water has a pronounced effect on the rates of formation of the peroxorhenium compounds; the reaction is fastest in water itself. We offer two plausible reasons for this effect: (a) the more polar solvent component would stabilize a polar transition state, and (b) water may also play a specific chemical role in the reaction, possibly by assisting proton transfer through a hydrogen-bonded intermediate. We shall examine each in turn. Kinetics data, including isotope effects and volumes of activation,[32] have been used to study the formation of **A**. It was concluded that this sequence applies:

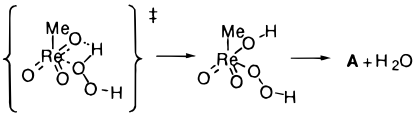

The transition state shown has bonds considerably more polar than in MTO and H_2O_2, suggesting that a kinetic acceleration arises from the general increase in polarity of the medium. Additionally, one or two water molecules may play an explicit chemical role in which hydrogen bonding to an intervening water molecule facilitates proton transfer in the step diagramed above. This idea is embodied in a modified transition state:

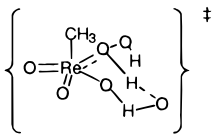

Thus it is not surprising to see a significant H_2O effect on the kinetics since formation and cleavage of O−H bonds are involved in the processes.

Solvent Effect on Organic Products. The *aqueous* decomposition of the MTO−H_2O_2 system in aqueous solution produces CH_3OH and ReO_4^-, not from **B**, but from a very fast reaction between MTO and HOO^-.[28] In organic media, however, the MTO−H_2O_2 system is more stable. To lower the deactivation rate of MTO−H_2O_2 in CD_3CN to about the same as that in aqueous solution would require that $[H^+]$ be increased to 5 M, there being an inverse rate effect on $[H^+]$ in water. The major organic product is CH_3OOH in CD_3CN and also in $CDCl_3$, CD_2Cl_2, acetone-d_6, and 2-propanol-d_8. Comparison of the product distributions in H_2O and CH_3CN solvents is given in Table 2.

The formation of CH_3OH in CD_3CN likely results from the reaction of MTO with HOO^-. The qualitative correlation between the amount of CH_3OH produced and the initial concentrations of H_2O_2 supports this contention. The large equilibrium constants and the small rate constants of the reverse reactions in acetonitrile suggest that very little rhenium species is present as MTO except at the beginning. About 60% of the total CH_3OH was observed in the first ^{1}H-NMR spectrum upon addition of H_2O_2 to the MTO solution, consistent with this assignment.

Scheme 1

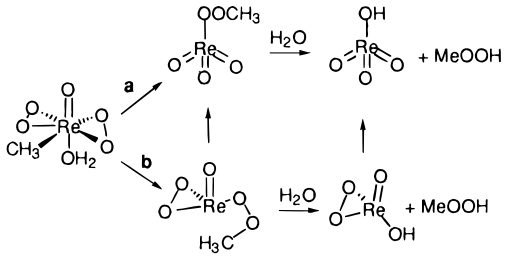

Mechanism for the Formation of CH_3OOH. The formation of CH_3OOH from **B** follows first-order kinetics with $k = 2 \times 10^{-6}$ s^{-1} at 25 °C. This rate constant is independent of the initial concentrations of **B** and H_2O_2. Scheme 1 was proposed to account for the observations of the formation of CH_3OOH and the unimolecular kinetic process. Coordinated water in Scheme 1 was omitted for clarity. The suggested derivatives, $CH_3OOReO(\eta^2\text{-}O_2)$ and CH_3OOReO_3, the later analogous to the known compound CH_3OReO_3, could be postulated. The literature reports that CH_3OReO_3 is moisture sensitive.[25] Indeed, we have shown that the addition of H_2O to a CD_3CN solution of CH_3OReO_3 produces CH_3OH promptly. It is reasonable to propose that CH_3OOReO_3 hydrolyzes CH_3OOH and $HOReO_3$. CH_3OOH may instead arise from the hydrolysis of $CH_3OOReO(\eta^2\text{-}O_2)$. Excess H_2O, introduced with 30% H_2O_2 used to prepare **B**, is inevitably present.

The key difference between the two proposed pathways is whether a Re^V or a Re^{VII} intermediate is involved. The concerted pathway, a, entangles many bond-breaking and -forming processes and seems to be unlikely, although the oxidation state of Re remains as VII throughout. Path b involving a $Re^V(d^2)-Re^{VII}(d^0)$ conversion, $CH_3OOReO(\eta^2\text{-}O_2)$ to CH_3OOReO_3 or $HOReO(\eta^2\text{-}O_2)$ to $HOReO_3$, is symmetry forbidden;[33] however, the formation of CH_3OOH is so slow that path b may indeed operate. The postulated thermal methyl migration to form rhenium methyl peroxide from **B** is different from the rearrangement proposed in the alkylperoxopermethyltantalocene system, eq 7. The conversion of $Cp^*_2Ta(\eta^2\text{-}O_2)(CH_3)$ to $Cp^*_2Ta(O)(OCH_3)$ at 80 °C occurs in a non-first-order fashion and is acid-catalyzed.[34] A concerted mechanism is preferred. On the other hand, the rearrangement in Scheme

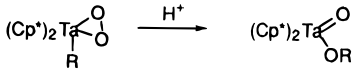

(7)

1 is similar to the $Cp^*_2Ta(\eta^2\text{-}CH_2O)(H)$ system, eq 8.[35] Instead of C−O bond cleavage concurrent with C−H bond formation, a stepwise process supported by the observation of an inverse kinetic deuterium isotope effect was proposed. Conversion of $Cp^*_2Ta(\eta^2\text{-}CH_2O)(H)$ to $Cp^*_2TaO(CH_3)$ obeys first-order kinetics with a rate constant of 3.03×10^{-6} s^{-1} at 140 °C, with an equilibrium between $Cp^*_2Ta(\eta^2\text{-}CH_2O)(H)$ and $Cp^*_2Ta(OCH_3)$.

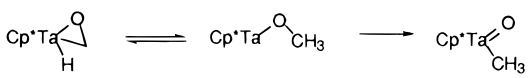

(8)

(32) Pestovsky, O.; van Eldik, R.; Huston, P.; Espenson, J. H. *J. Chem. Soc., Dalton Trans.* **1995**, 133.

(33) Brown, S. N.; Mayer, J. M. *Inorg. Chem.* **1992**, *31*, 4091.

(34) Van Asselt, A.; Trimmer, M. S.; Henling, L. M.; Bercaw, J. E. *J. Am. Chem. Soc.* **1988**, *110*, 8254.

(35) Van Asselt, A.; Burger, B. J.; Gibson, V. C.; Bercaw, J. E. *J. Am. Chem. Soc.* **1986**, *108*, 5347.

Scheme 2

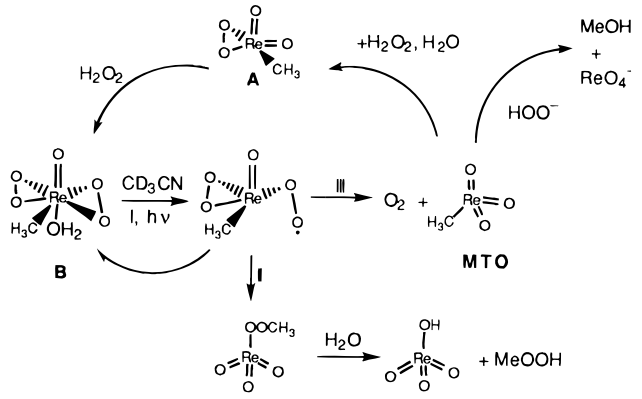

If the mechanism involved $CH_3^{\bullet}$, then CH_3OOH might be formed from $CH_3^{\bullet}$ with O_2 and subsequent hydrogen-atom abstraction. The lack of effect of molecular oxygen and the large activation entropy (-190 J mol^{-1} K^{-1}) of the decomposition processes rule out possible homolytic cleavage of the Re$-$$CH_3$ bond.

The rate constant for the decomposition of **B** to MeOOH *in acetonitrile* is 2×10^{-6} s^{-1}, nearly 150 times as large as the rate constant for its decomposition to O_2 *in water*, $k_9 = 2.9 \times 10^{-4}$ s^{-1}, both at 25 °C (eq 9). The solvent effect is quite large,

$$CH_3Re(O)(O_2)_2OH_2 \rightarrow CH_3ReO_3 + O_2 + H_2O \qquad (9)$$

sufficient to change not only the rate constant but the entire course of the reaction. No oxygen evolution was detected in acetonitrile, although the method is not too sensitive. If as much as 10% O_2 would have escaped detection, then in acetonitrile $k_9 < 2 \times 10^{-7}$ s^{-1}. The original issue, that methyl hydroperoxide is favored so much over oxygen in acetonitrile, becomes two others: How is it that MeOOH becomes favored over MeOH? This was addressed in the preceding paragraphs. And why is the rate constant for O_2 evolution favored so strongly in the one solvent? The strong solvent dependence for other MTO reactions comes to mind: the previously-discussed reaction of **B** to release **A** and hydrogen peroxide, $k_{-2} = 4 \times 10^{-2}$ s^{-1} and 7×10^{-5} s^{-1}, which is similar to the increase in k_9 (rate ratios are 600 and 1500). The key to understanding both lies in the role played by hydrogen bonding to stabilize the terminal O atom or OH group of an intermediate in which the atom bonded to rhenium is only one O atom (or OH group) of the incipient O_2 or H_2O_2 molecules. With this picture in mind, higher rates in water are easily understood.

Photolysis of B. CH_3OH and CH_3OOH are not interconverted thermally or photochemically under the experimental conditions, meaning that they arise independently. The first step in Scheme 2 consists of homolytic cleavage of a Re$-$O bond, as proposed in many photoinduced reactions involving metal peroxo complexes, though exceptions are known.[23,36] For example, the photocleavage of the O$-$O bond instead of a M$-$O bond has been proposed in the photochemical reactions of peroxotitanium(IV) porphyrin.[23] The experimental results in the case of the diperoxorhenium system could not conclusively rule out the O$-$O cleavage pathway; however, the formation of CH_3OOH and theoretical calculations on the analogous complex do favor the M$-$O cleavage pathway. Extended Hückel calculations are in favor of the homolysis of a Mo$-$O bond in the (TPP)Mo(η^2-O_2)$_2$ and the (HMPA)MoO(η^2-O_2)$_2$·H_2O systems upon photolysis.[22,37] The molecular orbital interaction diagram of **B** would be similar to that of (HMPA)-MoO(η^2-O_2)$_2$(H_2O). As a result, the absorption band around 360 nm for **B** is corresponding to a d $\leftarrow$ π^* (O_2^{2-}) transition. When the pentagonal plane is designated *xy*, cleavage of the Re$-$O (η^2-O_2) bond must result from the transition of the in-plane π^* (O_2^{2-}) orbitals to the d_{xy} or $d_{x^2-y^2}$ orbital. Whether a $CH_3^{\bullet}$ is also formed as a result will be discussed below.

Step II consists of a methyl migration followed by an intramolecular redox process. Unlike the thermal reaction, the methyl rearrangement need not cleave the Re$-$O bond. As a result, this process is much faster than the thermal methyl migration.

The elimination of molecular oxygen, step III, has been well documented in photochemical reactions involving metal peroxo complexes. As mentioned previously, $CH_3ReO(\eta^2\text{-}O_2)(\eta^1\text{-}OO^{\bullet})$ resulting from Re$-$O bond cleavage may be responsible for the formation of CH_3OOH. However, the generation of O_2 may not be from the same excited state if the O$-$O bond cleavage product, $CH_3ReO(\eta^2\text{-}O_2)(\eta^1\text{-}O^{\bullet})_2$, could also be produced upon photolysis. The electronic state of molecular oxygen was not determined in these studies, but $^3O_2$ was produced in CH_2Cl_2.[19] Since MTO is also formed as each oxygen molecule is released, decomposition of MTO to CH_3OH will compete with equilibration. The formation of CH_3OH and equilibration between MTO, **A**, and **B**, shown in the top part of the scheme, resemble the aqueous reactions. The product distribution ([CH_3OH] > [CH_3-OOH]), Table 2, suggests that the rates of steps III and II would be comparable.

Cleavages of the Re$-$O (η^2-O_2) and Re$-$$CH_3$ bonds upon photolysis of **B** in CH_2Cl_2 with 248$-$365 nm light were proposed.[19] Chloromethane was observed. The energies of the light sources were in the range of 328$-$482 kJ mol^{-1}, which are probably larger than the unknown Re$-$$CH_3$ bond energy. In our studies, the photolysis energy was lower, <299 kJ mol^{-1}, but still larger than the energy of one of the strongest transition metal carbon bonds, Ta$-$$CH_3$ ($D_{Ta-C} = 261$ kJ mol^{-1}).[38] The photoproducts from **B** in CD_3CN under Ar are the same as those under O_2, but a mechanism involving a free methyl radical still could not be ruled out since O_2 was produced upon irradiation of **B**. However, to date the only detected products from the reaction of $CH_3^{\bullet}$ with O_2 in the literature are CH_3OH, CH_2O, and CH_3OOCH_3,[39] in contrast to CH_3OH and CH_3OOH observed in the photolysis of **B**. The photoproducts from **B** in CD_2Cl_2 at >400 nm are different from those at 248$-$365 nm, suggesting that $CH_3^{\bullet}$ is not likely involved in the photolysis of **B** at >400 nm.

Photocatalysis. One of our goals was to investigate the possibility of using **B** as a photocatalyst. As indicated in Scheme 2, the use of an oxygen-centered radical $CH_3ReO(\eta^2\text{-}O_2)(\eta^1\text{-}OO^{\bullet})$, generated from the initial photolysis step, was limited owing to step II. To trap $CH_3ReO(\eta^2\text{-}O_2)(\eta^1\text{-}OO^{\bullet})$, 1,4-dihydronaphthalene was used. The results are indicative but not conclusive on this point. Phenoxyl radicals were suggested by the oxygen-dependent photoreactions with 2,4,6-trialkylphenols. The stability of the phenoxyl radical could be the driving force for the reaction of $CH_3ReO(\eta^2\text{-}O_2)(\eta^1\text{-}OO^{\bullet})$ with ArOH. Rearrangement of $ArO^{\bullet}$ to a carbon-centered radical and its subsequent reaction with oxygen are known.[40] The low yields

(36) Peterson, M. W.; Van Atta, R. B.; Richman, R. M. *Inorg. Chem.* **1983**, *22*, 1982.
(37) Ledon, H. L.; Bonnet, M. *J. Am. Chem. Soc.* **1981**, *103*, 6209.
(38) Adedeji, F. A.; Connor, J. A.; Skinner, H. A.; Galyer, L.; Wilkinson, G. *J. Chem. Soc., Chem. Commun.* **1976**, 159.
(39) Simon, F.-G.; Schneider, W.; Moortgat, G. K. *Int. J. Chem. Kinet.* **1990**, *22*, 791.
(40) Altwicker, E. R. *Chem. Rev.* **1967**, *67*, 475.

were discouraging as far as the prospects for photocatalysis go, and the matter was not pursued further.

Conclusion. Water affects the rates and equilibria of the $MTO-H_2O_2$ system in CH_3CN, more for the formation of **A** than **B**. Although the $MTO-H_2O_2$ system is much more stable in organic solvents than water, the generation of the real oxo-transfer catalysts, **A** and **B**, is much slower in organic solvents than in water. This may be a consequence of the direct involvement of water in the mechanism of peroxide binding. The decomposition of **B** produces CH_3OOH in acetonitrile but CH_3OH in aqueous solution. Light facilitates the decomposition processes, but **B** is not a likely photocatalyst given its rapid conversion to CH_3OOH.

Acknowledgment. This work was supported by a grant from the National Science Foundation (CHE-9007283). Some of the experiments were conducted with the use of the facilities of the Ames Laboratory.

IC970650C